Symbolic dynamics of the hyperbolic potential

Wei-Mou Zheng
Institute of Theoretical Physics, Academia Sinica, Beijing 100080, China
(Received 15 May 1997)

An appropriate Poincaré surface of section without referring to bounce events is introduced for the x^2y^2 potential. By means of the map on the annulus and the lifted space the symbolic dynamics of the system is constructed. Symmetries are used to reduce the number of symbols. [S1063-651X(97)13810-7]

PACS number(s): 05.45.+b, 03.20.+i

By the hyperbolic potential system we mean the Hamiltonian [1]

$$H=\frac{1}{2}(p_x^2+p_y^2+x^2y^2), \tag{1}$$

which appears in the long-wavelength limit of SU(2) Yang-Mills theory [2]. After regularization by conversion to the semiparabolic coordinates [3] a hydrogen atom in a magnetic field or a collinear helium atom can be described by similar Hamiltonians [4,5]. Being invariant under the group C_{4v}, the Hamiltonian (1) possesses rotational and reflectional symmetries, and is similar to the symmetric four disk billiard. The three-letter alphabet {0,1,2} coding for billiard orbits is well known [1,4]. Based on bounce events in the symmetric four disk billiard, code 2 is assigned to a diagonal bounce (i.e., a scattering from a disk to the disk diagonal to it), code 1 to a nondiagonal bounce of an equal sense with its last nondiagonal bounce, and code 0 to a nondiagonal bounce of an opposite sense. If a correspondence between orbits of a billiard and those of the hyperbolic potential exists, we may code orbits of the hyperbolic potential according to bounces. However, bounces are not always well defined for a soft potential like x^2y^2, and no Poincaré surface of section defined according to bounces is available. In this paper we shall introduce a Poincaré section appropriate for the hyperbolic potential and describe its symbolic dynamics.

The rotational symmetry can be easily described for a map on the annulus. Consider the contour shown in Fig. 1, which starts at the positive infinity of the x axis and goes along both x and y axes in the counterclockwise direction. We may convert the contour into a circle with a circumference of 8. Each straight segment of the contour then corresponds to a nonoverlapping arc of length 1 on the circle. The specific form of the transformation from the contour to a circle is not essential to our discussion. The transformation we use is defined as follows. Denote by s the arc length on the circle measured from the point $(s=0)$ corresponding to the point $(x,y)=(+\infty,0^+)$ on the contour. The transformations for the eight straight segments of the contour in the counterclockwise order are $1/(1+x)$, $2-1/(1+y)$, $2+1/(1+y)$, $4-1/(1-x)$, $4+1/(1-x)$, $6-1/(1-y)$, $6+1/(1-y)$, and $8-1/(1+x)$.

Imagining that the x and y axes would be of a finite width, we may define the inside of the contour. By recording the nonvanishing coordinate and the tangent component v of the momentum at crossing points where an orbit enters the contour, the Poincaré map can be obtained. On the corresponding circle contour, the map represents a map on the annulus. Let us define the fundamental domain (FD) of the annulus to be the area of $s\in[0,8)$ and $v\in[-1,1]$. For a map on the annulus it is useful to consider its lift [6–9]. In the lifted space on which the lift map is defined the image of the FD is partly sketched in Fig. 2 where the FD is the rectangle consisting of the leftmost eight strips marked with the numbers 0 to 7. In the figure we draw only the images of strips 1 and 2. Two zones marked with 1 and $1'$ of strip 1 are mapped to zone 1 of strip $+3$ and zone $1'$ of strip $+2$, respectively. The notation representing the image of strip 2 is analogous. The rotational symmetry of the Hamiltonian (1) corresponds to the translational symmetry in the lifted space. For example, the image of strip 0 is in strips 6 and 7, and can be obtained from the image of strip 2 (in the strips $+0$ and $+1$) by shifting to the left by two strips.

For the full FD, the rotation number of orbits is between 0 and 2. Taking the rotational symmetry into account, we may consider only the reduced domain (RD) consisting of strips 1 and 2. When the RD is regarded as the annulus, from Fig. 2 the integral part of rotation numbers is 3, 4, or 5 for zone 2,

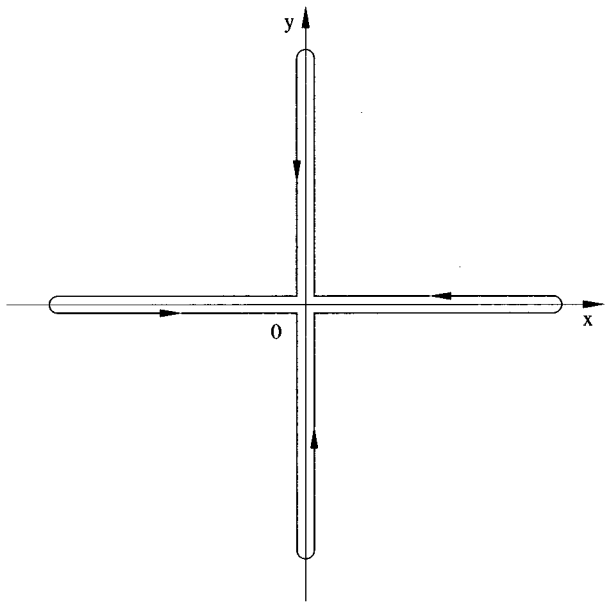

FIG. 1. Contour for the Poincaré surface of section.

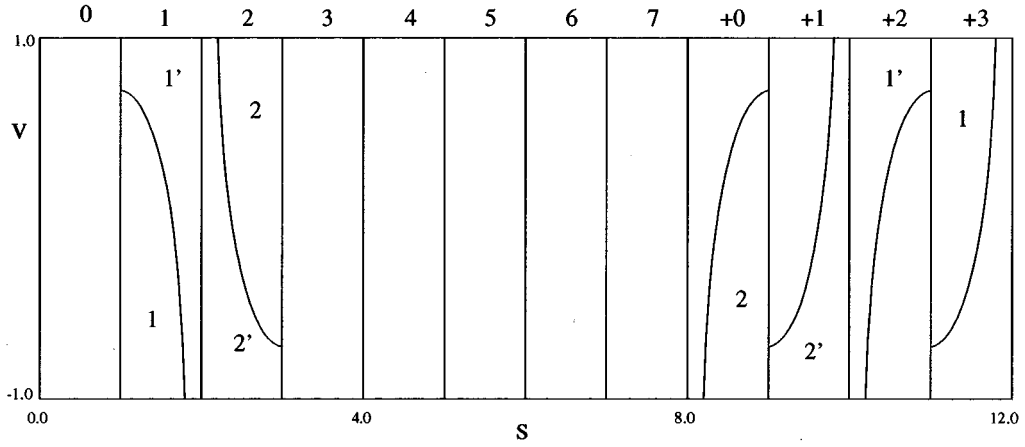

FIG. 2. Sketch showing the image of the fundamental domain.

the joint zone $1'$ and $2'$ or zone 1, respectively. The RD is correspondingly divided into three regions according to the rotation number. In the RD, tangencies between stable and unstable manifolds can be easily seen. Among them, the prominent ones are in zones 1 and 2. At a given point the stable and unstable directions or tangent directions of manifolds can be determined with the procedure suggested by Greene [10], and then tangent points found. Two lines connecting such tangent points, which go approximately along nearby stable manifolds, give a further partition of the RD. The final partition of the RD into five regions is sketched in Fig. 3 where these regions are marked by $\bullet L_0$, $\bullet R_0$, $\bullet R_1$, $\bullet R_2$, and $\bullet L_2$. In the figure the two boundaries of the RD are marked with $\bullet D_0$ and $\bullet D_2$, the two lines of tangencies by $\bullet C_0$ and $\bullet C_2$, and two other lines separating different rotation numbers, being the preimage of $\bullet D_0$ or $\bullet D_2$, are marked by $\bullet B_0$ and $\bullet B_2$. By means of this partition we may code an orbit with a doubly infinite sequence

$$\cdots s_{-1}\bullet s_0 s_1 \cdots,$$

where $\bullet$ indicates the present.

The ordering is essential to the construction of symbolic dynamics. We may accept the natural order of the lifted space to write

$$\bullet L_0 < \bullet R_0 < \bullet R_1 < \bullet R_2 < \bullet L_2. \tag{2}$$

From the image of the RD shown in Fig. 2 we see an opposite arrangement of the image zones in the lifted space. A more precise description of ordering is given by the ordering of stable manifold foliations on a transversal unstable foliation. It is numerically verified that under the forward map the ordering is reversed in the regions $\bullet R_0$, $\bullet R_1$, and $\bullet R_2$, but preserved in $\bullet L_0$ and $\bullet L_2$. We may define the parity of a finite string by the oddness of the total number of the letters R_0, R_1, and R_2 contained in the string. Any odd leading string will then reverse the ordering (2).

The image of the partition shown in Fig. 3 gives the partition according to preimages. The study of this partition under the backward map provides the information about the ordering of backward sequences. Similarly, we have

$$L_0\bullet < R_0\bullet < R_1\bullet < R_2\bullet < L_2\bullet, \tag{3}$$

and an odd leading string also reverses this ordering. Here the ordering rules for forward and for backward sequences coincide. However, generally they are different. The stadium billiard is an example [9].

Based on the ordering rules, metric representations for both forward and backward sequences may be introduced to construct the symbolic plane [11]. Every forward or backward sequence then corresponds to a number between 0 and 1. An orbit point corresponds to a point (α,β) in the unit square, where α and β are associated with the forward and backward sequences, respectively. In the symbolic plane forbidden sequences are pruned by the so-called primary prun-

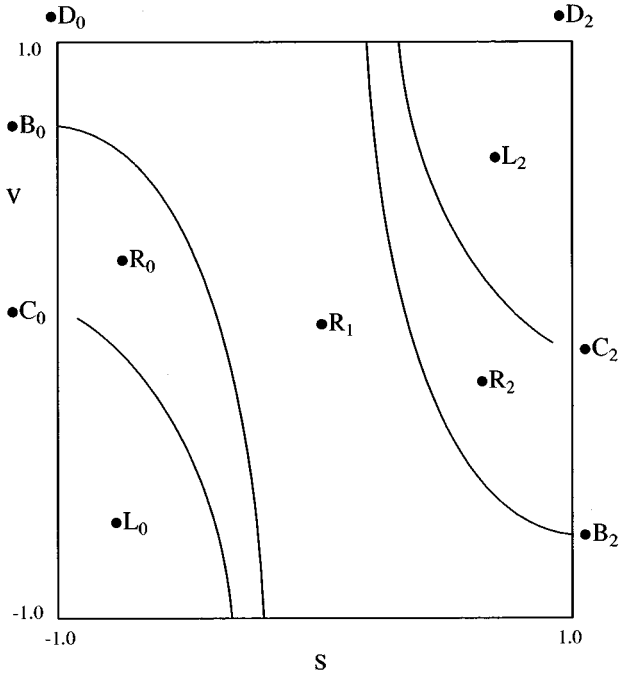

FIG. 3. Sketch showing the partition of the reduced domain. We have used an equivalent range $[-1.0,1.0)$ for s instead of $[1.0,3.0)$.

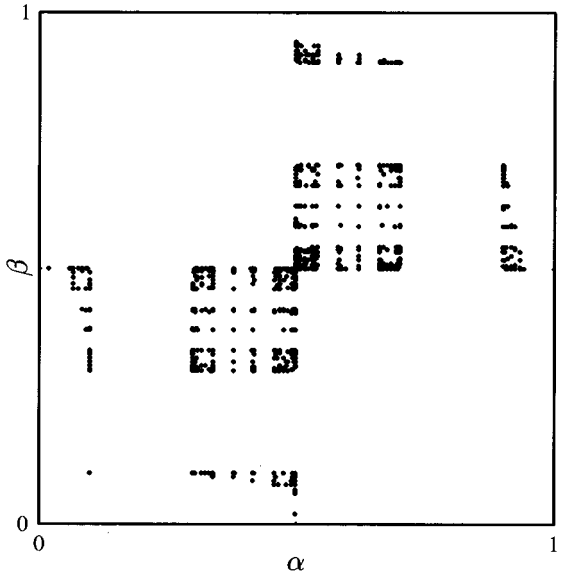

FIG. 4. Symbolic plane of the reduced domain. Approximately 6 000 real orbit points are drawn.

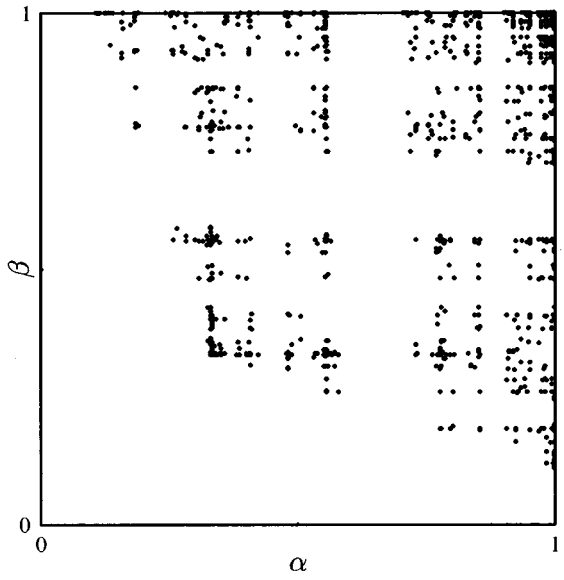

FIG. 6. Symbolic plane of the minimal domain. Approximately 6 000 real orbit points are drawn.

ing front which consists of the points in the symbolic plane representing all the points on the partition lines $\bullet D_0$, $\bullet D_2$, $\bullet C_0$, and $\bullet C_2$. We show the symbolic plane of the x^2y^2 potential in Fig. 4 where 6 000 points of several real orbits are drawn. The corresponding primary pruning front is shown in Fig. 5.

So far we have not considered the reflectional symmetry. In fact, the second and fourth quadrants in the symbolic plane are forbidden by the symmetry. In the lifted space this symmetry corresponds to the invariance of the RD under a π rotation around the center (or the reflection with respect to the center). From Fig. 2 it is seen that the image of zone 1 of strip 1 is in strip $+3$, hence still in 1 after wrapping. On the contrary, the image $1'$ of strip 1 is in strip 2. However, the π rotation can put the image back into strip 1. So, using the reflectional symmetry, we may focus only on strip 1, which may be regarded as the minimal domain (MD). In this way the five-letter symbolic dynamics is reduced to the three-letter one, and the π rotation changes the parity of R_1. More specifically speaking, we have the following ordering for the minimal domain:

$$\bullet L_0 < \bullet R_0 < \bullet R_1, \quad L_0 \bullet < R_0 \bullet < R_1 \bullet, \tag{4}$$

and only R_0 in a leading string reverses the ordering. The symbolic plane of the MD is shown in Fig. 6 where 6 000

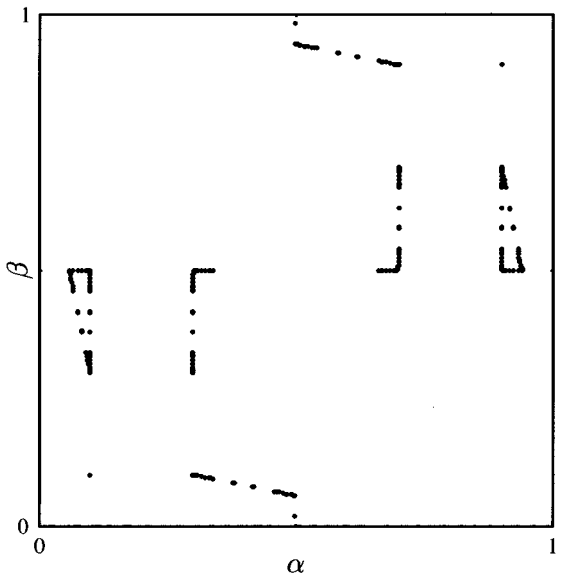

FIG. 5. Primary pruning front of the reduced domain. It forms the border of the region within which orbit points are restricted to fall.

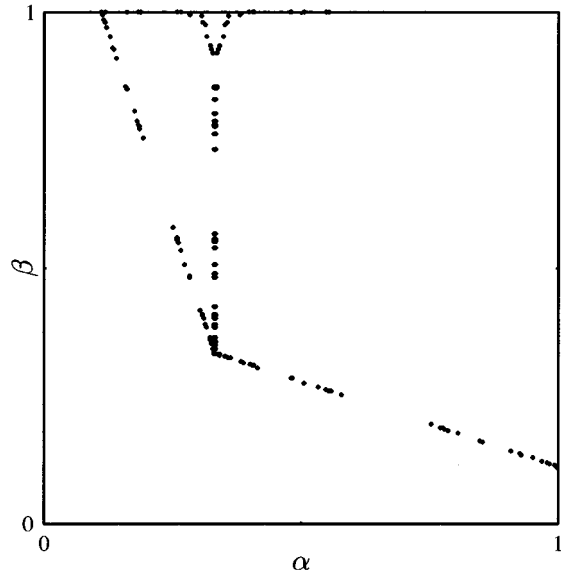

FIG. 7. Primary pruning front of the minimal domain. It forms the border of the region within which orbit points are restricted to fall.

points of several real orbits are drawn. The corresponding primary pruning front is shown in Fig. 7 where the pruning front of $\bullet D_0$ is roughly diagonal, while that of $\bullet C_0$ is almost vertical. The latter encloses a forbidden zone near the top in the symbolic plane, which is responsible for many interesting bifurcations, e.g., the one mentioned in Ref. [1] associated with the orbits $(210)^\infty$ and $(1000)^\infty$ in their codes [or $(L_0R_1^3)^\infty$ and $(R_0R_1^3)^\infty$ in our codes]. Finally, we give examples of different codings for some orbits shown in Ref. [1]:

{0,1,2}-code	five-letter code	three-letter code
220^5	$R_1L_0R_1L_2R_1^6L_2R_1L_0R_1^5$	$R_1L_0R_1L_0R_1^5$,
01010^5	$R_1R_0R_1R_2R_1^6R_2R_1R_0R_1^5$	$R_1R_0R_1R_0R_1^5$,
20^5	$D_0^2R_1^4B_0D_2^2R_1^4B_2$	$D_0^2R_1^4B_0$,
110^5	$R_0^2R_1^5R_2^2R_1^5$	$R_0^2R_1^5$,
110^6	$R_0^2R_1^6$	$R_0^2R_1^6$.

Note that the first two orbits which have the same topology may be distiguished in our code since the first orbit has L_0 and L_2 instead of R_0 and R_2, respectively.

In the above we have given a natural way to construct symbolic dynamics for the x^2y^2 potential. Our choice of the Poincaré section avoids any ambiguity in identifying bounces. A lift of the phase space helps us to understand the dynamics. Tangencies between stable and unstable manifold foliations play an important role in the construction of symbolic dynamics. Our discussions are specifically made only for the x^2y^2 potential, but the arguments may be applied to other systems such as the n-disk pinballs, a hydrogen atom in a magnetic field [12], a collinear helium atom, and the anisotropic Kepler system as well. Discussion on symbolic dynamics and bifurcation behavior of these systems will be presented elsewhere.

The author thanks Hao Bai-lin and K.T. Hansen for useful discussions. This work was supported in part by the National Natural Science Foundation of China.

[1] P. Dahlqvist and G. Russberg, J. Phys. A **24**, 4763 (1991).
[2] S.G. Matanyan, G.K. Savvidy, and N.G. Ter-Arutyunyan-Savvidy, Sov. Phys. JETP **53**, 421 (1981).
[3] S.J. Aarseth and K. Zare, Celest. Mech. **10**, 185 (1974).
[4] B. Eckhardt and D. Wintgen, J. Phys. B **23**, 353 (1990).
[5] K. Richter, G. Tanner, and D. Wintgen, Phys. Rev. A **48**, 4182 (1993).
[6] D.K. Arrowsmith and C.M. Place, *An Introduction to Dynamical Systems* (Cambridge University Press, Cambridge, 1990).
[7] J.D. Meiss, CHAOS **2**, 267 (1992).
[8] I. Percival and F. Vivaldi, Physica D **27**, 373 (1987).
[9] W.M. Zheng, Phys. Rev. E **56**, 1556 (1997).
[10] J.M. Greene, in *Long-Time Prediction in Dynamics*, edited by W. Horton, L.E. Reichl, and V. Szebehely (Wiley, New York, 1983).
[11] P. Cvitanović, G.H. Gunaratne, and I. Procaccia, Phys. Rev. A **38**, 1503 (1988).
[12] K.T. Hansen and S. Güttler, J. Phys. A (to be published).